19th Australasian Fluid Mechanics Conference
Melbourne, Australia
8-11 December 2014

# CFD Simulation and FE Analysis of a High Pressure Ratio Radial Inflow Turbine

**M. Odabaee, M. Modir Shanechi and K. Hooman**
School of Mechanical and Mining Engineering
University of Queensland, Queensland, 4072, Australia

## Abstract

The present study investigates a coupled CFD&FE analysis of a high pressure ratio single stage radial-inflow turbine applied in the Sundstrans Power Systems T-100 Multipurpose Small Power Unit. ANSYS turbomachinary package is applied to create 3D geometry of one blade passage, including the stator, rotor and diffuser. CFD simulations are performed with ANSYS-CFX in which three-dimensional Reynolds-Averaged Navier-Stokes equations are solved subject to appropriate boundary conditions. CFD results are then imported to ANSYS Steady-State Thermal and Static Structural module enabling thermal stress and blade deformation analysis. The von Mises stress $\sigma_v$ distribution is calculated by means of finite element analysis (FEA). Centrifugal forces acting on the turbine wheel are considered along with thermal stresses. Once validated against available experimental data, numerical (CFD-FEA) results are extended to cases where no experimental data could be found in the literature allowing for better understanding of the performance of such radial inflow turbines at higher rpms where significant centrifugal forces can affect the integrity of the turbine.

## Introduction

Concentrated solar power can play a significant role in generating electrical power. In such systems, the sunlight is concentrated thereby increasing the working fluid temperature and associated power conversion efficiencies. The Supercritical Carbon dioxide ($sCO_2$) Bryton cycle has emerged as a promising path for high-efficiency power production. Hence, the turbomachinery for $sCO_2$ Brayton is being developed [7]. This study is conducted to validate the code and turbine simulation progress towards the simulation of a supercritical $CO_2$ radial-inflow turbine which will be designed, manufactured and tested in future as a part of the Australian Solar Thermal Research Initiative.

In order to predict turbine characteristics, it is essential to compute flow field throughout the turbine, analyse the flow passage where viscous three dimensional rotational/curvature and turbulence effects play significant roles. Although there are few published experimental studies on radial turbines [5, 6, 19, 8], a well-documented experimental work on thermo-mechanical analysis of such turbine with a supercritical fluid flowing through it is yet to be reported. CFD simulations have been, nonetheless, conducted to achieve a better understanding of the flow characteristics, including grid refinements and independency, and the validation of numerical results (1D & 3D) as discussed in [15, 18, 3, 12, 2, 13, 1]. Considering the numerical simulations on radial-inflow turbines available in the literature, the necessary geometric pieces of information are not available in published documents. Therefore, one cannot reproduce the same exact geometry to conduct CFD simulations [17].

However, Sauret [17] provided a fully open set of data and recreated the exact geometry of the high pressure ratio single stage radial-inflow turbine used in [8]. The study includes a preliminary 1D design using RITAL checked against Hamilton Sundstrand and available experimental data [8]. The 3D geometry was created in Axcent with rotor and stator blade profiles as well as thicknesses and angles details. Axcent-PushButton CFD was then applied to solve the 3D viscous flow simulations where the effect of the tip clearance gap was investigated for a range of operating conditions.

Aiming at decreasing apparent stress, Yonghui et al. [9] presented an optimisation method using finite element structural analysis. Furthermore, [11] investigated blade vibration for a high-speed centrifugal compressor to avoid blade failure caused by an excessive resonant response. Moreover, as the geometrical parameters are strongly coupled, and both the aerodynamic and structural issues coexist, an iterative design procedure is called for.

Mueller and Alsalihi [10] presented a two-level optimisation algorithm by means of accurate steady state 3D Navier-Stokes and centrifugal stress computations. Their results showed that a smaller blade leading edge meridional length improved both the aero-performance and moment of inertia. Studying the trailing edge meridional length, those authors reported that there was an optimum exit flow area as a result of a trade-off between the aero-performance and the moment of inertia. This is mainly because, a large trailing edge results in improved efficiency, while the shortening that edge reduces the moment of inertia. Considering the stress analysis, it was observed that reducing the blade thickness minimises the moment of inertia with negligible impact on the aero-performance.

An investigation on aerodynamic performance, structural strength, blade geometry, and wheel weight was presented by Fu et al [4] to develop an optimisation design approach for radial turbine with 230 *mm* rotor inlet diameter considering material characters, shafting and bearing load capacity, manufacturing, and installation technology. Employing their integrated optimisation design method including CFD and FE analysis, the main structural modelling parameters of rotor such as leading and trailing meridional lengths, blade thickness and angle distribution, as well as tip clearance were reselected to reduce the weight.

Following the geometrical data provided in [17], the present study recreates the 3D geometry of the identical turbine applying commercially available software ANSYS to conduct a numerical simulation for the rig conditions. The results are compared with numerical and experimental data presented in [17, 8]. Furthermore, the simulation was extended to cases where no experimental data were available.

## 3D Geometry

To define the 3D geometry of the turbine, ANSYS-BladeGen was used to recreate the 3D nozzle and rotor blades, as shown in figures 1 and 2. The geometrical data from [17] including nozzle hub and shroud thicknesses (similar on hub and shroud), nozzle

blade profile (adjusted by Piecewise linear curves), rotor hub and shroud contours and rotor blade angle and thickness distributions for both hub and shroud separately (adjusted by Piecewise linear curve) were applied in order to define an identical turbine. The 3D diffuser geometry was generated using ANSYS-Geometry separately, considering the correct dimensions of the diffuser. The tip clearance in the original design decreases linearly from 0.4 *mm* at the leading edge to 0.23 *mm* at the trailing edge, which is not a state-of-the-art value for this impeller, despite having a smart linear distribution.

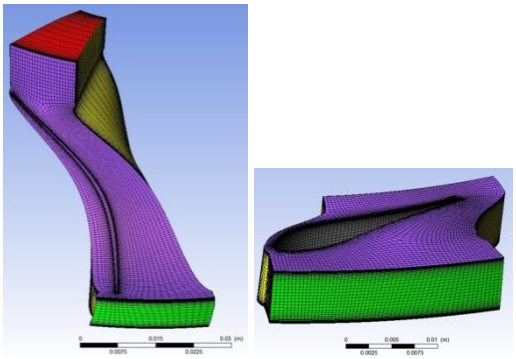

Figure 1. 3D view of mesh generated for rotor (left) and stator (right) blade flow passage, presenting inlet( green), outlet (red), shroud (purple) and periodic surfaces (yellow).

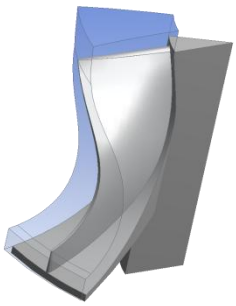

Figure 2. 3D view of rotor flow passage besides solid region including hub and shaft.

## Numerical Simulation

To reduce the computational cost in this design approach, only one section of the turbine wheel is modelled and periodic boundary conditions are applied for both the fluid and the solid domain.

### Discretization

ANSYS-TurboGrid was applied to generate the flow passage meshes for both rotor and stator where the Automatic Topology and Meshing (ATM Optimized) option was used in stator and rotor flow passages. For the boundary layer refinement control, the first element method was used with Near Wall Element Size Specification to meet the $y^+$ requirement for the turbulence model, ranging from 6 to 147. After checking grid refinement and mesh quality, the total grid number is 748484 -including stator, rotor, and diffuser- where the final mesh analysis of rotor and stator flow passages shows 30º for minimum face angle, 155º for maximum face angle with a positive minimum volume.
Structural mechanics simulations needed to use the mesh efficiently as run times can be impaired with high element counts. ANSYS Meshing has a physics preference setting ensuring the right mesh for each simulation. The solid geometry for the stress analysis is discretised with hybrid grids, quadratic tetrahedral elements, with a local refinement in the blade fillets to resolve the high stress loading in this region. The total number of elements is kept around 200,000 to satisfy the mesh-independent criterion.

### Solvers and Boundary Conditions

The mesh from ANSYS-TurboGrid was imported into ANSYS CFX to conduct the 3D viscous flow simulations. SST turbulence model was chosen as recommended by [16, 14]. The basic settings used for the discretisation of the Reynolds-Averaged Navier-Stokes (RANS) equations - for a steady state solution - are High Resolution Advection Scheme and High Resolution Turbulence Numerics. The inlet total pressure, inlet total temperature and outlet static pressure of rig condition are defined and set in CFX-Pre. The operating pressure and temperature of the rig condition are 413.6 *kPa* and 477.6 *K*, respectively[17].
To evaluate the strength performance accurately, ANSYS Structural module is adopted in the present modelling and the von Mises stress distribution is determined. The turbine wheel is made of a superalloy with the mass density of ~7810 $kg/m^3$. Inconel 792 nickel-base superalloy, a cast high-strength polycrystalline material designed for the production of blades and discs of gas turbine engines for use at temperatures up to 950°C, is selected as the material. At high temperature conditions (900°C), Young's modulus and poisson's ratio of material are 169 *GPa* and 0.4, respectively.
The rotational speed (71700 *RPM*) and same free displacement of the 1/16 rotor wheel section are imposed in the FEA computation. The aforementioned material characteristics with respect to corresponding temperature also are taken into account during FEA calculation. The obtained temperature and pressure distributions are imported from fluid module to the solid module in order to calculate effect of thermal stress and pressure load as induced by aerodynamic forces. Both direct and iterative solvers are adopted and results show no significant difference.

## Results and Discussions

3D contours of static temperature and pressure through stator and rotor flow passage are presented in figure 3. As shown in Figure 3.a, the highest static temperature occurs at the stator inlet, decreasing throughout stator and rotor flow passages and reaches its minimum value of 302 *K* at the rotor outlet. The static pressure distribution is shown in figure 3.b where it reduces from 413 *kPa* to 67.323 *kPa* at the stator entrance and rotor exit, respectively.

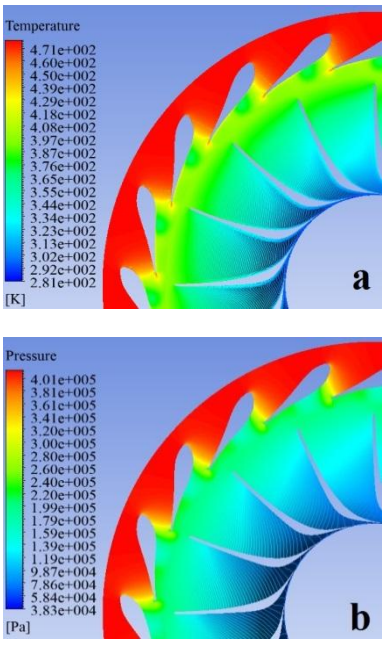

Figure 3. a) Static temperature and b) static pressure distribution on stator and rotor flow passage at span 0.5.

Total-to-static and total-to-total efficiencies are presented in table 1 comparing the results of CFX to those of experimental investigations conducted in [8]. Note that CFD predictions for our efficiencies between the stator inlet and diffuser outlet and the generated power are within 2% of the measured data. The rotational speed was increased to 106588 *RPM* to observe CFD results of the design condition (meanline design) with the same pressure ratio, see more details in [8, 17]. CFD results of higher rotational speed predict almost identical efficiencies and power compared to those of meanline design.

| | CFD | Experiments |
|---|---|---|
| Total-to-static efficiency [%] | 84 | 86.4 |
| Total-to-total efficiency [%] | 85.3 | 87.7 |
| Power [*kW*] | 36.4 | 36.7 |

Table 1. Comparison of numerical with experimental efficiencies.

The distribution of von Mises stress of the turbine wheel is shown in figure 4. It has a high stress value of 522 *MPa* located at the blade root section where the maximum blade thickness is designed to be on the hub. The lowest stress value of 0.08 *MPa* is noted at the leading edge and tip shroud close to the trailing edges. Figure 5 illustrates the deformation distribution of the rotor where the maximum value of 0.1 *mm* is predicted at the tip and a 0.08 *mm* deformation is expected at the leading edges in line with the experimental results reported in [8] where the tip clearance was 0.23 *mm* to leave enough space for tip deformation from leading edge to the trailing edge.

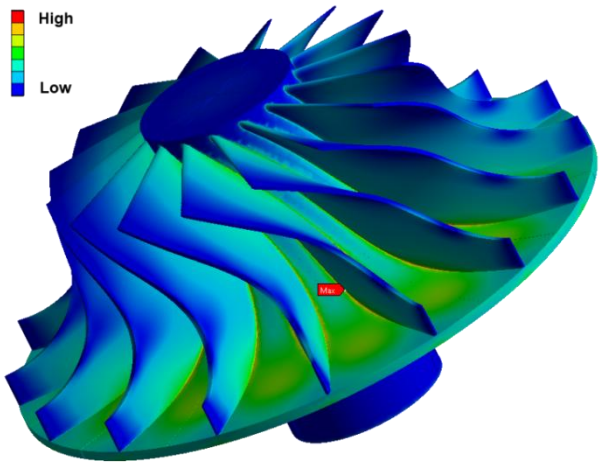


Figure 4. 3D counter of stress distribution, maximum is 522 *MPa*.

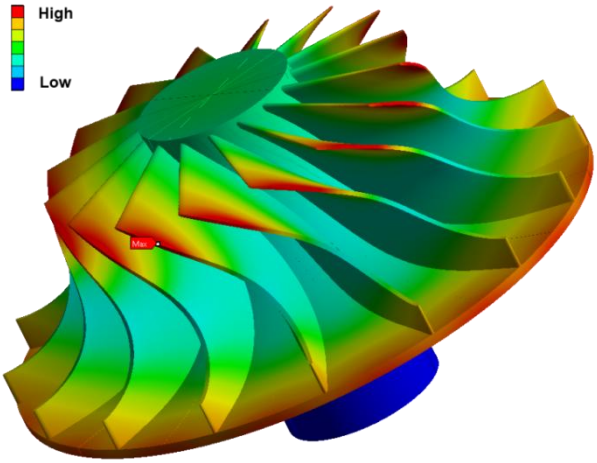


Figure 5. 3D counter of deformation distribution, maximum is 0.1 *mm*.

## Conclusions

The aim of the present study is to reproduce the closest geometry of a high pressure ratio single stage radial-inflow turbine applied in the Sundstrans Power Systems T-100 Multipurpose Small Power Unit by using CFD & FEA tools. A numerical simulation was performed where the 3D RANS and the von Mises stress distribution equations were solved. The proposed design of the turbine is carefully examined against the published geometrical data and results confirm that the correct 3D geometry is successfully reproduced. The comparisons between numerical and experimental results show a good agreement with experimental data.

## Acknowledgments

This research was performed as part of the Australian Solar Thermal Research Initiative (ASTRI), a project supported by the Australian Government, through the Australian Renewable Energy Agency (ARENA).

## References

[1] Carrillo, R.A.M., et al., *RADIAL INFLOW TURBINE ONE AND TRI-DIMENSIONAL DESIGN ANALYSIS OF 600 kW SIMPLE CYCLE GAS TURBINE ENGINE*. Proceedings of the Asme Turbo Expo 2010, Vol 5. 2010, New York: Amer Soc Mechanical Engineers. 477-486.

[2] Choi, H.-J., et al., *CFD validation of performance improvement of a 500 kW Francis turbine.* Renewable Energy, 2013. 54(0): p. 111-123.

[3] Deng, Q.H., et al., *Experimental and numerical investigation on overall performance of a radial inflow turbine for 100kw microturbine*. Proceedings of the Asme Turbo Expo, Vol 3. 2007, New York: Amer Soc Mechanical Engineers. 919-926

[4] Fu, L., et al., *Integrated Optimization Design for a Radial Turbine Wheel of a 100 kW-Class Microturbine.* Journal of Engineering for Gas Turbines and Power, 2011. 134(1): p. 012301-012301.

[5] Hiett, G. and I. Johnston. *Experiments concerning the aerodynamic performance of inward flow radial turbines*. in *Proceedings of the Institution of Mechanical Engineers*. 1936.

[6] Holeski, D.E. and M.G. Kofskey, *Cold performance evaluation of a 6.02-inch radial inflow turbine designed for a 10-kilowatt shaft output Brayton cycle space power generation system*, in *NASA Technical Report*. 1966, NASA Lewis Research Center; Cleveland, OH, United States.

[7] Iverson, B.D., et al., *Supercritical CO2 Brayton cycles for solar-thermal energy*. Applied Energy, 2013. 111(0): p. 957-970.Jones, A.C., Design and Test of a Small, High Pressure Ratio Radial Turbine. Journal of Turbomachinery, 1996. 118(2): p. 362-370.

[8] Jones, A.C., *Design and Test of a Small, High Pressure Ratio Radial Turbine*. Journal of Turbomachinery, 1996. 118(2): p. 362-370.

[9] Kishor Kumar, et al. *Design and Analysis of a High Pressure Turbine Using Computational Methods for Small Gas Turbine Application*. in *ASME 2013 Gas Turbine India Conference*. 2013. Bangalore, Karnataka, India: ASME Proceedings

[10] Lasse Mueller, Zuheyr Alsalihi, and T. Verstraete, *Multidisciplinary Optimization of a Turbocharger Radial Turbine.* Journal of Turbomachinery, 2012. 135(2): p. 9.

[11] Lei Huang, et al. *Numerical Investigation of the Effect of Rotor Blade Leading Edge Geometry on the Performance of a Variable Geometry Turbine*. in *ASME Turbo Expo 2012: Turbine Technical Conference and Exposition*. 2012. Copenhagen, Denmark: ASME Proceedings.

[12] Lewis Research, C. and A.J. Glassman, *Computer program for design analysis of radial-inflow turbines*. 1976, Washington, D.C. : [Springfield, Va.: National Aeronautics and Space Administration ; For sale by the National Technical Information Service].

[13] Li, Y.J., Q. Zheng, and Asme, *Numerical simulation of a multistage radial inflow turbine*. Proceedings of the ASME Turbo Expo 2006, Vol 6, Pts A and B. 2006, New York: Amer Soc Mechanical Engineers. 1141-1148.

[14] Louda, P., et al., *Numerical simulation of turbine cascade flow with blade-fluid heat exchange.* Applied Mathematics and Computation, 2013. 219(13): p. 7206-7214.

[15] Prasad, V., *Numerical simulation for flow characteristics of axial flow hydraulic turbine runner.* Energy Procedia, 2012. 14(0): p. 2060-2065.

[16] Rocha, P.A.C., et al., *k–ω SST (shear stress transport) turbulence model calibration: A case study on a small scale horizontal axis wind turbine.* Energy, 2014. 65(0): p. 412-418.

[17] Sauret, E., *Open Design of High Pressure Ratio Radial-Inflow Turbine For Aacademic Validation*, in *ASME 2012 International Mechanical Engineering Congress & Exposition*. 2012: Houston, Texas, USA.

[18] Simpson, A.T., S.W.T. Spence, and J.K. Watterson, *Numerical and Experimental Study of the Performance Effects of Varying Vaneless Space and Vane Solidity in Radial Turbine Stators.* Journal of Turbomachinery, 2013. 135(3): p. 031001-031001.

[19] Stephen Spence and D. Artt, *Experimental performance evaluation of a 99.0 mm radial inflow nozzled turbine with different stator throat areas.* Proceedings of the Institution of Mechanical Engineers, Part A: Journal of Power and Energy, 1997. 211(A6): p. 477-488.